https://doi.org/10.20965/ijat.2015.p0612

Review:

Fabrication Process of Antimony Telluride and Bismuth Telluride Micro Thermoelectric Generator

Mizue Mizoshiri*, Masashi Mikami, and Kimihiro Ozaki****

*Graduate School of Engineering, Nagoya University
Furo-cho, Chikusa-ku, Nagoya, Aichi 464-8603, Japan
E-mail: mizoshiri@mech.nagoya-u.ac.jp
**National Institute of Advanced Industrial Science and Technology
2266-98 Anagahora, Moriyama-ku, Nagoya, Aichi 463-8560, Japan
[Received June 4, 2015; accepted October 1, 2015]

This paper describes the process of fabricating micro thermoelectric generators (μ-TEGs) based on antimony telluride (Sb-Te) and bismuth telluride (Bi-Te). These materials have excellent thermoelectric (TE) conversion properties. The deposition and patterning processes for thermoelectric films are key techniques in the fabrication of μ-TEGs. However, it is difficult to form TE micropatterns using conventional semiconductor technologies because Sb-Te and Bi-Te are brittle and difficult to etch. Therefore, a semiconductor fabrication process is developed for TE film patterning. Here, various processes for depositing Sb-Te and Bi-Te TE films are described. Then, the combinations of the deposition and patterning techniques are reviewed. Finally, the generation properties of the μ-TEGs are summarized.

Keywords: micro thermoelectric generator, bismuth-telluride film, sputtering, lithography, lift-off process

1. Introduction

Thermoelectric (TE) generation is an energy harvesting technology that converts ambient thermal energy to electric energy. Thermoelectric generators (TEGs) are composed of a number of p- and n-type TE element couples that are connected in series. When a temperature gradient (temperature difference) is generated between the hot side and the cold side of the p-n junctions, the generation voltage V and maximum power P_{Max} can be expressed using Eqs. (1) and (2).

$$V = \int_{T_c}^{T_h} \{S_p(T) - S_n(T)\} dT \cdot N \approx \{\tilde{S}_p - \tilde{S}_n\} \Delta T \cdot N \quad \ldots\ldots\ldots\ldots\ldots\ldots\ldots\ldots (1)$$

$$P_{Max} = \left[\{V_p - V_n\} \Delta T \cdot N\right]^2 R_L/(R+R_L)^2 \quad (2)$$

Here, S_i, T_h, T_c, ΔT, R_L, R, and N are the Seebeck coefficient of the TE elements, the hot side temperature, the cold side temperature, the temperature difference, the load resistance, the internal resistance of the generator, and the number of pn junctions, respectively. The generation voltage increases in proportion to the difference in temperature. The increase in power equals the square of the difference between the two temperatures. In general, it is difficult to generate a large temperature gradient using a small amount of thermal energy in an ambient atmosphere. However, the relatively large voltage needed can be generated by increasing the number of p-n junctions. Therefore, micro thermoelectric generators (μ-TEGs) are useful because the micro-sized TE film elements can be densely integrated.

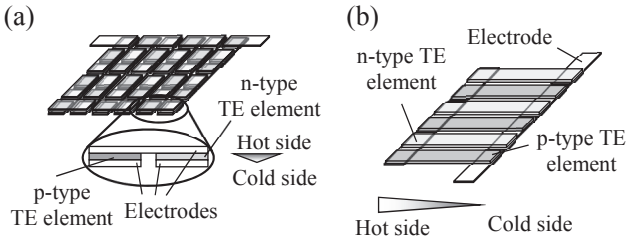

Fig. 1. Two types of μ-TEGs: (a) vertical and (b) planar.

As shown in **Fig. 1**, μ-TEGs are classified into two types, a vertical type and a planar type, according to their structures. The vertical μ-TEGs have the same structures as conventional bulk TE modules. The temperature difference has to be generated in the TE film thickness direction. It is difficult to generate the large temperature difference needed within the micro-sized length, but the TE elements can be densely integrated. In the planar μ-TEGs, the temperature difference is generated in the planar direction. The density of the TE elements is lower than it is in μ-TEGs, but a relatively large temperature difference can be generated between the hot side and cold side of pn junctions by controlling the length of the elements.

To date, various TE materials, including Sb-Te, Bi-Te, poly-Si, Skutterudite, and Heusler alloys, have been developed, and their use in the fabrication of the TE modules has been demonstrated [1–4]. The TE conversion is characterized by the figure of merit $ZT(=S_i^2 T/\rho\kappa)$ using the Seebeck coefficient S_i, the temperature T, the electrical resistivity ρ, and the thermal conductivity κ. S_i^2/ρ is a power factor which exhibits maximum generation power and is also commonly used to exhibit the generation properties. Sb-Te and Bi-Te are two excellent ma-

terials, exhibiting large figures of merit (~ 1) in low temperature ranges. However, Sb-Te and Bi-Te μ-TEGs cannot be fabricated using well-established semiconductor technologies, such as lithography, deposition, and etching processes, as these processes have mainly been developed for Si-based semiconductor microfabrication [5, 6]. Consequently, the fabrication process of Sb-Te and Bi-Te-based μ-TEGs has been studied by many researchers. In this paper, we focus on the fabrication process of Sb-Te and Bi-Te-based μ-TEGs. To fabricate these μ-TEGs, the TE material depositions and their patterning processes are key technologies. Furthermore, the various combinations of those processes are also important. First, the fabrication processes of the μ-TEGs are reviewed. Then, the patterning processes which take into account the deposition processes are presented. Finally, the generation properties of the μ-TEGs are summarized.

2. Deposition Process of Antimony Telluride and Bismuth Telluride Films

2.1. Co-Evaporation Deposition

The evaporation technique is a simple vacuum deposition process. However, it is difficult to control the composition ratio of Sb-Te and Bi-Te by using the material alloys themselves as the raw materials. This is because the vapor pressure of Te is significantly higher (more than 10^4 times) than those of Bi and Sb. To solve this problem, the co-evaporation technique was used [7–9]. In the co-evaporation deposition of Bi-Te materials, for example, Bi and Te were simultaneously evaporated by individually controlling the evaporation conditions in order to deposit materials of the desired composition. The raw materials which evaporated at low pressure (approximately $10^{-3} - 10^{-4}$ Pa) were deposited on the substrates. Stoichiometric p-type Sb_2Te_3 and n-type Bi_2Te_3 thin films were deposited on glass substrates [8]. When the substrate temperatures of p-type Sb_2Te_3 and n-type Bi_2Te_3 were kept at approximately 503 K and 533 K, respectively, the Seebeck coefficient and electrical conductivity of Sb_2Te_3 and Bi_2Te_3 were 185 μV/K, $0.32 \times 10^3 \Omega^{-1}$ cm^{-1} and -228 μV/K, and $0.77 \times 10^3 \Omega^{-1}$ cm^{-1}, respectively. Both Sb_2Te_3 and Bi_2Te_3 films were polycrystalline. Furthermore, the Bi_2Te_3 films showed a preferential orientation along the c-axis. This higher electrical conductivity in the planar direction is an advantage of planar μ-TEGs.

Other groups have investigated the dependence of thermoelectric material properties on deposition conditions, such as substrate temperature, substrate materials, and composition ratio [9]. A comparison of the X-ray diffraction patterns (XRD) of Bi_2Te_3 films deposited at 403 K and 533 K on glass substrates has revealed that the film deposited at 533 K has a preferential orientation along the c-axis while that deposited at 403 K has random polycrystallinity. When Bi_2Te_3 films were deposited at 533 K on various substrates, such as soda lime glass, Al_2O_3 (0001), MgO (100), mica, and Pt substrates, (00l) and (015) planes were observed on all substrates. However, the crystals grown on mica, Pt, and Al_2O_3 were more randomly oriented. The film deposited on the glass substrate, which exhibited a higher level of orientation along the c-axis, exhibited the highest level of electrical conductivity. These results are in line with the results in other reports. The composition ratio of Te affected the Seebeck coefficient and the electrical conductivity. By taking these parameters into account, a higher figure of merit was obtained in the case of 60 at.%-Te. For Sb_2Te_3 depositions, the differences between the maximum and minimum Seebeck coefficients at various substrate temperatures were lower, which means that the sensitivity of the Sb and Te composition ratio was lower than that of the Bi and Te compound.

2.2. Sputtering Deposition

The sputtering deposition technique is useful in depositing Bi-Te and Sb-Te because almost the same composition ratios of the sputtering targets and deposited films are obtained [10–13]. Radio frequency (RF) magnetron sputtering [10] was used to deposit Bi-Te films. In the RF co-sputtering deposition, Bi-Te thin films were deposited by individually controlling the sputtering conditions of the Bi and Te targets [11]. The maximum Seebeck coefficient of stoichiometric Bi_2Te_3 thin film was -55 μV/K when the substrate temperature was 498 K.

The raw powders are directly used as the sputtering targets [12]. Bi and Te powders were mixed and placed on non-magnetic discs. The compositions of the deposited films were easily controlled by verifying the ratio of the powder mixture.

P-type $Bi_{0.5}Sb_{1.5}Te_3$ and n-type $Bi_2Te_{2.7}Se_{0.3}$ films were deposited by RF and direct current magnetron sputtering [13, 14]. The Seebeck coefficient and electrical conductivity of these films are excellent, much better than those of stoichiometric Sb_2Te_3 and Bi_2Te_3 films.

Deposition by means of sputtering is effective, as previously mentioned. However, the deposition rate of Sb-Te and Bi-Te was as small as 0.03–0.14 μm/min. To increase the deposition rate of the films, the thermally assisted sputtering method (TASM) was developed [15]. This technique is based on a direct current magnetron sputtering method. A higher deposition rate was achieved by increasing the temperature of the target because the sputter yield of materials increases as material temperature increases. To increase the temperature of the target, the target was isolated from the cooling system for the magnets under the target. This was done by inserting a temperature-control spacer between the target and the backing plate. The maximum deposition rate of Sb_2Te_3 and Bi_2Te_3 thick films on glass substrates was approximately 1.6 μm/min when the temperatures of the Sb_2Te_3 and Bi_2Te_3 targets were 536 K and 563 K, respectively. The differences in the composition ratios between the deposited films and Sb_2Te_3 and Bi_2Te_3 targets were less than 3.6% and 1.5%, respectively. The maximum thickness of the films was approximately 100 μm, as shown in **Fig. 2**.

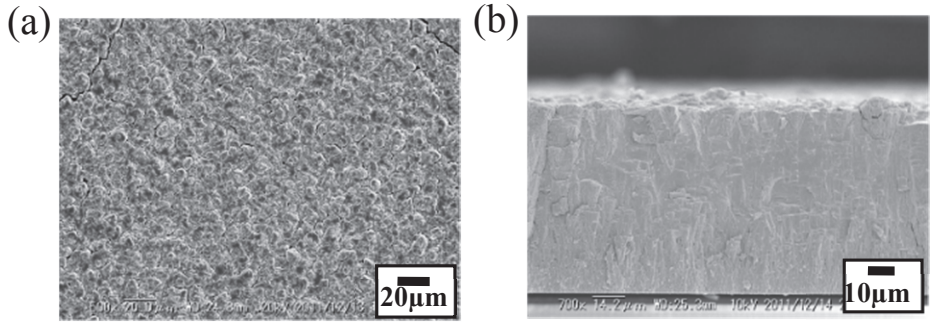

Fig. 2. SEM images of (a) the surface and (b) cross-section of Bi_2Te_3 thick film [15].

Table 1. Thermoelectric properties of the deposited films.

Deposition method	Co-evaporation [8]	Sputter [14]	Electro chemical [17]	Print [21]
Seebeck coefficient (μV/K)	$185/-228$	$191/-201$	$/-63$	$174/-287$
Electrical conductivity(Ω^{-1}cm^{-1})	320/770	29/455	$-/-$	532/775
Power factor (μW/cmK^2)	11/40	1/18	$-/-$	16/64

The Seebeck coefficients of Sb_2Te_3 and Bi_2Te_3 films were 180 μV/K and -150 μV/K, respectively, almost the same as those of conventional sputtered films.

2.3. Electrochemical Deposition

The electrochemical deposition process has been widely studied because it has the advantages of higher deposition rate, easily-controllable deposition thickness, and low cost [16, 17]. Sb_2Te_3 films were deposited on a Pt/Si substrate and an Au seed layer [16]. The electrolyte solutions consisted of $HTeO_2^+$ and SbO^+. As-deposited amorphous Sb_2Te_3 films were annealed to improve crystallinity. XRD patterns of the as-deposited and annealed films indicated an improvement in crystallinity afforded by the annealing process. Furthermore, there was preferential orientation in the [015] direction. This result agreed with the substrate dependence, as mentioned in section 2.1 [9].

Other groups have also reported on the electrochemical deposition of Bi_2Te_3 films. Single-phase Bi-Te films were deposited using electrolyte solutions of Bi_2O_3 and TeO_2 in diluted HNO_3. The Bi_2Te_3 films exhibited a preferential orientation along the *c*-axis [17]. The maximum Seebeck coefficient was -63 μV/K.

2.4. Printing and Coating Deposition

Printing technology is the combination process of deposition and patterning steps. Some researchers have reported on the printing and coating of Sb-Te and Bi-Te films.

P-type $Bi_{0.4}Te_3Sb_{1.6}$ films have been fabricated using nanoparticles with an average size of approximately 50 nm [19]. A 1-μm thick layer of nanoparticles mixed with toluene and surfactant was spin-coated on an Al_2O_3 substrate. Then, the films were sintered in the temperature range of 573 K to 773 K in a hydrogen atmosphere for 60 min. The Seebeck coefficient decreased and the electrical conductivity increased with increases in the sintering temperature. When the Seebeck coefficient of the thin film was 65 μV/K and the electrical conductivity was 109 Ω^{-1} cm^{-1} while the sintering temperature was 623 K, the maximum thermoelectric power factor was 1.3 μW/cmK^2. The thermoelectric properties of the printed films depended on the particle size [20]. When the particle diameters were 0.66 and 2.8 μm, the Seebeck coefficient of the films were 42 μV/K and 79 μV/K, respectively. On the contrary, the electrical conductivity of the films with 0.66 μm-particles was as much as 420 Ω^{-1} cm^{-1} higher than that of the films with 2.8 μm-particles.

N-type Bi_2Te_3 and p-type Sb_2Te_3 thick films were also prepared using printing technology [21]. Sb_2Te_3 and Bi_2Te_3 powders were milled to produce 10 μm average particles. The powders were dispersed in epoxy resin systems. Then, the glass substrates were coated with inks and cured at temperatures from 423 K to 573 K. The maximum Seebeck coefficient of p-type Sb_2Te_3-epoxy and n-type Bi_2Te_3-epoxy composite films were 174 μV/K at a 473 K curing temperature and -287 μV/K at a 623 K curing temperature.

2.5. Thermoelectric Properties of the Deposited Films

Table 1 shows the thermoelectric properties of the films deposited by various deposition methods. The films deposited under vacuum or reduction atmospheres exhibit relatively higher Seebeck coefficients and electrical conductivities. Unfortunately, the value of the Seebeck coefficient of Sb-Te films deposited by means of electrochemical deposition could not be obtained, even though the deposition properties obtained when the electrochemical method was used have been reported. It might be more difficult to obtain a large Seebeck coefficient of Sb-Te films by using the electrochemical deposition method than by using Bi-Te deposition.

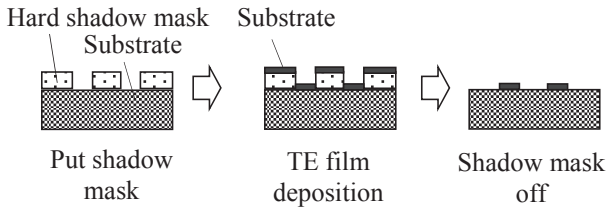

Fig. 3. Schematic illustration of the patterning process using hard shadow mask and deposition.

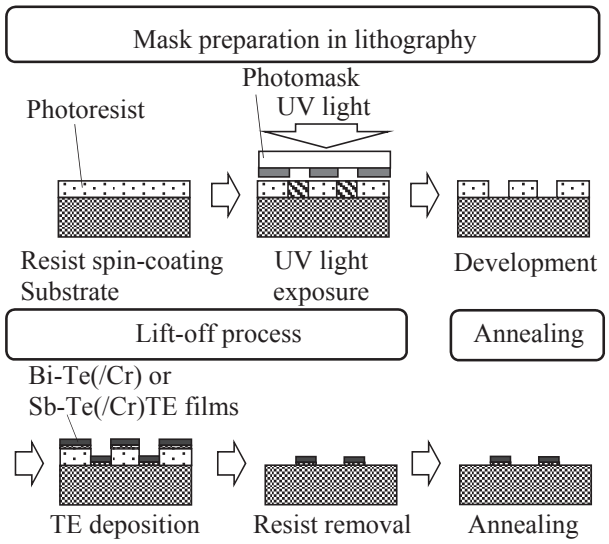

Fig. 4. Schematic illustration of a process combining the lithography and the lift-off technique.

3. Patterning Processes of Thermoelectric Films

3.1. Hard Shadow Mask Patterning Processes

The hard shadow mask process is a simple patterning process. **Fig. 3** is a schematic illustration of the patterning process. The substrates were covered with hard metal masks when the thermoelectric film was deposited using vacuum processes, such as co-evaporation and the sputtering method. After the deposition, the hard masks were removed from the substrate. This process has an advantage over the lithography method in that it uses low-heat-resistance photopolymer as the mask. This is because the substrate can be heated during the deposition. In section 2, the substrate temperature is an important parameter in the deposition of Bi-Te and Sb-Te films with excellent thermoelectric properties, such as its Seebeck coefficient and electrical conductivity properties. The hard shadow mask materials are generally stainless steel films approximately 1-mm thick. Therefore, the masks are not damaged by the substrate temperature of approximately 500 K. Sb_2Te_3 and Bi_2Te_3 films were deposited by co-evaporation and patterned using hard shadow masks [21].

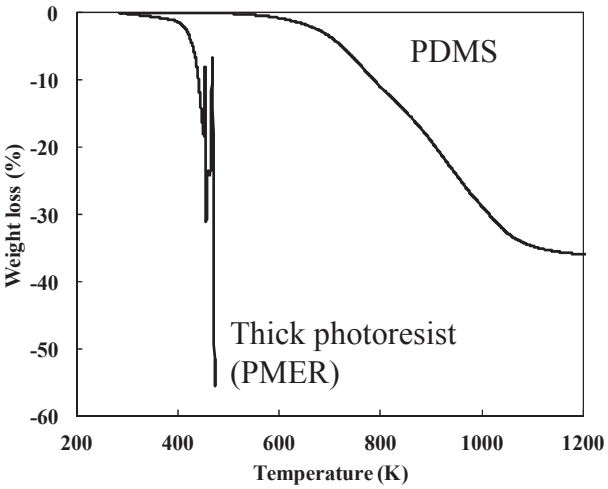

Fig. 5. Thermogravimetric curves of PDMS and thick photoresist [26].

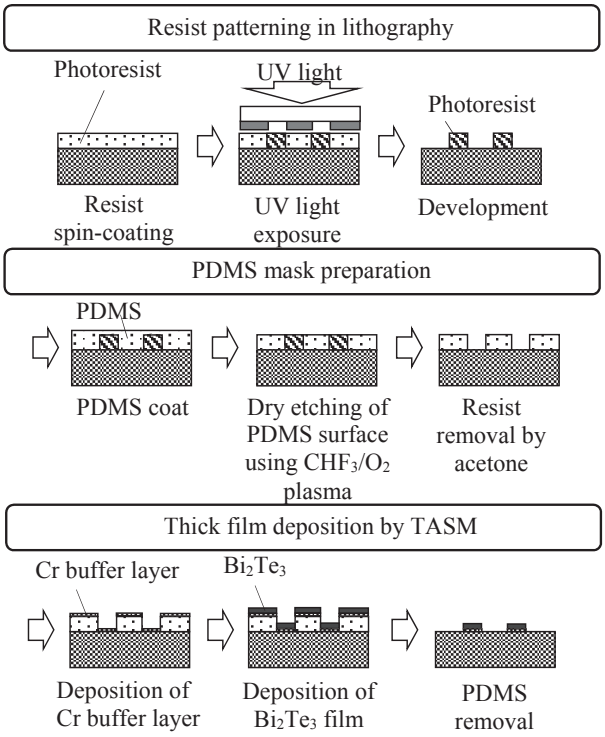

Fig. 6. Schematic illustration of fabrication process of planar μ-TEGs using TASM and lift-off techniques [26].

3.2. Lithography and Lift-Off Process

One well-known microfabrication technique is a combination of the lithography and lift-off processes. **Fig. 4** is a schematic illustration of a combination of the lithography and lift-off techniques. When the thermoelectric films were deposited by the co-evaporation and sputtering methods, the substrate temperature could not be increased because the resist patterns, which are photosensitive polymers in the lift-off process, exhibited low heat-resistance properties. Therefore, the thermoelectric film deposition was carried out without substrate heating [15, 22–26]. The patterned thermoelectric films were then annealed af-

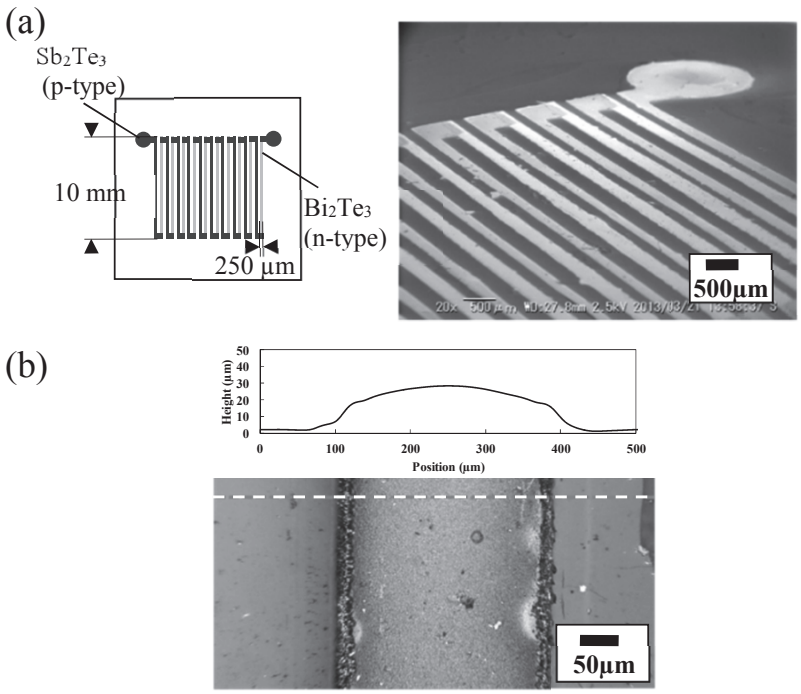

Fig. 7. (a) SEM image of thermoelectric module pattern of Sb_2Te_3 (p-type) and Bi_2Te_3 (n-type) elements, and (b) optical microscope image and the cross-sectional profile of the pattern [26].

ter the resist removal. To date, planar-type thermoelectric films with 10 pairs of pn junctions have been fabricated using this process [15, 24, 25]. To improve the adhesion of p-type $Bi_{0.5}Sb_{1.5}Te_3$ and n-type $Bi_2Te_{2.7}Se_{0.3}$ thermoelectric films to the glass substrate, a 1-nm Cr buffer layer was inserted between the thermoelectric films and the glass substrates [25].

More heat-resistant lift-off masks that use silicone materials (poly(dimethylsiloxane, PDMS)) to form patterns of thick films deposited by TASM have also been reported [26]. In TASM, the substrate temperature increases as the temperature of the target increases, so it is difficult to use conventional photoresist patterns. **Fig. 5** shows the thermal properties of the PDMS that were evaluated using thermogravimetric analysis. A chemically-amplified positive tone photoresist is shown as a reference for comparison. PDMS exhibits significant weight loss at 553 K although the photoresist starts to show weight loss at 323 K.

Figure 6 is a schematic illustration of the fabrication processes of the μ-TEGs. First, PDMS mask patterns were formed using lithographic patterned resists, dry etching of PDMS, and resists removed by acetone. Then, Bi_2Te_3 thick films were deposited on the substrate with PDMS mask patterns. Finally, the PDMS patterns were removed. **Fig. 7(a)** is a schematic illustration and SEM image of a planar μ-TEG. An optical microscope image and cross-sectional profile of the Bi_2Te_3 thick film elements are shown in **Fig. 7(b)**.

3.3. Lithography and Etching Process

Compared to materials conventionally used in semiconductor technologies, Sb-Te and Bi-Te materials are more difficult to etch using dry and wet etching processes. However, a few research studies have reported a μ-TEG fabrication process that uses a combination of lithography and etching techniques. A schematic illustration of the fabrication processes is presented as **Fig. 8**. First, Sb-Te and Bi-Te thermoelectric films are deposited using deposition processes. Here, the substrate can be heated during deposition because no low thermal materials, such as photoresist patterns, are deposited on the substrates. Then, the resist patterns are formed on the thermoelectric films by means of the lithographic process. Following that, the thermoelectric films are etched using an HCl/HNO_3 mixed solution [8, 27, 28].

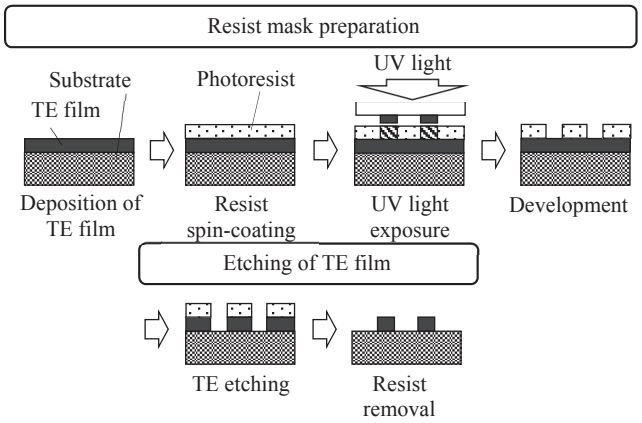

Fig. 8. Schematic illustration of the combination process of lithography and etching steps.

4. Generation Properties of Micro Thermoelectric Generator

Ambient thermal energies, such as waste heat, body energy, and solar energy, were used for generation. The μ-TEG with a number of pn junctions generated electric energy using light [22]. The generation voltage and the maximum generation power were approximately 4 mV and 1 μW, respectively. The temperature gradient was also generated using focused solar light [13, 24]. When all solar energy was used for thermoelectric conversion, the generation voltage and generation power of the μ-TEGs were 140 mV and 0.7 μW, respectively. A photo-thermoelectric hybrid generator was also fabricated [24]. Focused infrared (IR) solar light, separated using a hot mirror, was used for thermoelectric generation. The remaining solar light without IR light was used for photovoltaic generation. The generation voltage and generation power of the μ-TEGs were 78 mV and 0.19 μW, respectively. Although the generation power was as low as the μ-watt order, the generation voltage was as high as the sub-volt order. The higher generation voltage is advantageous for electric charge to batteries. Using a combination of the μ-TEGs with batteries, these methods of power generation can be used as energy harvesting devices [28].

5. Conclusion

This article has focused on the fabrication processes and the generation properties of μ-TEGs. Various deposition and patterning processes for TE films have been developed. The combinations of the processes are important for the fabrication of μ-TEGs.

References:

[1] M. Kishi, H. Nemoto, T. Hamao, M. Yamamoto, S. Sudou, M. Mandai, and S. Yamamoto, "Micro thermoelectric modules and their application to wristwatches as an energy source," Eighteenth International Conference on Thermoelectrics Proceedings, ICT'99, pp. 301-307, 1999.

[2] M. Nishibori, W. Shin, K. Tajima, L. F. Houlet, N. Izu, I. Matsubara, and N. Murayama, "Catalyst combustors with B-Doped SiGe/Au thermopile for micro-power-generation," Jpn. J. Appl. Phys., Vol.45, pp. L1130-L1132, 2006.

[3] J. Q. Guo, H. Y. Geng, T. Ochi, S. Suzuki, M. Kikuchi, Y. Yamaguchi, and S. Ito, "Development of Skutterudite Thermoelectric Materials and Modules," J. Electron. Mater., Vol.41, pp. 1036-1042, 2012.

[4] M. Mikami, K. Kobayashi, T. Kawada, K. Kubo, and N. Uchiyama, "Development and Evaluation of High-Strength Fe_2VAl Thermoelectric Module," Jpn. J. Apl. Phys., Vol.47, pp. 1512-1516, 2008.

[5] J. Xie, C. Lee, M.-F. Wang, Y. Liu, and H. Feng, "Characterization of heavily doped polysilicon films for CMOS-MEMS thermoelectric power generators," J. Micromech. Microeng., Vol.19, pp. 125029-1-125029-8, 2009.

[6] S. M. Yang, T. Lee, and M. Cong, "Design and verification of a thermoelectric energy harvester with stacked polysilicon thermocouples by CMOS process," Sens. And Actuators, A157, pp. 258-266, 2010.

[7] L. M. Goncalves, C. Couto, P. Alpuim, A. G. Völklein, and J. H. Correia, "Optimization of thermoelectric properties on Bi_2Te_3 thin films deposited by thermal co-evaporation," Thin Solid Films, Vol.518, pp. 2816-2821, 2010.

[8] H. Zou, D. M. Rowe, and G. Min, "Preparation and characterization of p-type Sb_2Te_3 and n-type Bi_2Te_3 thin films grown by coevaporation," J. Vac. Sci. Technol. A, Vol.19, pp. 899-903.

[9] L. W. da Silva, M. kaviany, and C. Uher, "Thermoelectric performance of films in the bismuth-tellurium and antimony-tellurium systems," J. Appl. Phys., Vol.97, pp. 114903, 2005.

[10] D.-H. Kim, S.-H. Lee, J.-K. Kim, and G.-H. Lee, "Structure and electrical transport properties of bismuth thin films prepared by RF magnetron sputtering," Appl. Surf. Sci., Vol.252, pp. 3525-3531, 2006.

[11] D.-H. Kim, E. Byon, G.-H. Lee, and S. Cho, "Effect of deposition temperature on the structural and thermoelectric properties of bismuth telluride thin films grown by co-sputtering," Thin Solid Films, Vol.510, pp. 148-153, 2006.

[12] H. Huang, W. Luan, and S. Tu, "Influence of annealing on thermoelectric properties of bismuth telluride films grown via radio frequency magnetron sputtering," Thin Solid Films, Vol.517, pp. 3731-3734, 2009.

[13] M. Mizoshiri, M. Mikami, K. Ozaki, and K. Kobayashi, "Thin-Film Thermoelectric Modules for Power Generation Using Focused Solar Light," J. Electron. Mater., Vol.41, pp. 1713-1719, 2012.

[14] D. Bourgault, C. G. Garampon, N. Caillault, L. Carbone, and J. A. Aymami, "Thermoelectric properties of n-type $Bi_2Te_{2.7}Se_{0.3}$ and p-type $Bi_{0.5}Sb_{1.5}Te_3$ thin films deposited by direct current magnetron sputtering," Thin Solid Films, Vol.516, pp. 8579-8583, 2008.

[15] M. Mizoshiri, M. Mikami, and K. Ozaki, "p-Type Sb_2Te_3 and n-Tyep Bi_2Te_3 Films for Thermoelectric Modules Deposited by Thermally Assisted Sputtering Method," Jpn. J. Appl. Phys., Vol.52, pp. 06GL07-1-06GL07-6, 2013.

[16] K. Park, F. Xiao, B. Y. Yoo, Y. Rheen, and N. V. Myung, "Electrochemical deposition of thermoelectric Sb_xTe_y thin films and nanowires," J. Alloys Compd., Vol.485, pp. 362-366, 2009.

[17] Y. Miyazaki and T. Kajitani, "Preparation of Bi_2Te_3 films by electrodeposition," J. Cryst. Growth, Vol.229, pp. 542-546.

[18] M. Takashiri, S. Tanaka, M. Takiishi, M. Kihara, K. Miyazaki, and H. Tsukamoto, "Preparation and characterization of Bi0.4Te3.0Sb1.6 nanoparticles and their thin films," J. Alloys Compd., Vol.462, pp. 351-355, 2008.

[19] K. Kato, H. Hagino, and K. Miyazaki, "Fabrication of Bismuth Telluride Thermoelectric Films Containing Conductive Polymers Using a Printing Method," J. Electron. Mater., Vol.42, pp. 1313-1318, 2013.

[20] D. Madan, A. Chen, P. K. Wright, and W. Evans, "Dispenser printed composite thermoelectric thick films for thermoelectric generator applications," J. Appl. Phys., Vol.109, pp. 034904-1-034904-6, 2011.

[21] B. Huang, C. Lawrence, A. Gross, G.-S. Hwang, N. Ghofouri, S.-W. Lee, H. Kim, C.-P. Li, C. Uher, K. Najafi, and M. Kaviany, "Low-temperature characteirzation and micropatterning of coevaporated Bi_2Te_3 and Sb_2Te_3 films," J. Appl. Phys., Vol.104, pp. 113710-1-113710-8, 2008.

[22] G. J. Snyder, J. R. Lim, C.-K. Huang, and J.-P. Fleurial, "Thermoelectric microdevice fabricated by a MEMS-like electrochemical process," Nature Mater., Vol.2, pp. 528-531, 2003.

[23] L. M. Goncalves, J. G. Rocha, C. Couto, P. Alpuim, G. Min, D. M. Rowe, and J. H. Correia, "Fabrication of flexible thermoelectric microcoolers using planar thin-film technologies," J. Micromech. Microeng., Vol.17, pp. S168-S173, 2007.

[24] M. Mizoshiri, M. Mikami, and K. Ozaki, "Thermal-Photovoltaic Hybrid Solar Generator Using Thin-Film Thermoelectric Modules," Jpn. J. Appl. Phys., Vol.51, pp. 06FL07-1-06FL07-5, 2012.

[25] M. Mizoshiri, M. Mikami, and K. Ozaki, "The effect of Cr buffer layer thickness on voltage generatioin of thin-film thermoelectric modules," Vol.23, pp. 115016-1-115016-9, 2013.

[26] M. Mizoshiri, M. Mikami, K. Ozaki, M. Shikida, and S. Hata, "Lift-off patterning of thermoelectric thick films deposited by a thermally assisted sputtering method," Appl. Phys. Express, Vol.7, pp. 057101-1-057101-4.

[27] L. M. Goncalves, C. Couto, P. Alpuim, and J. H. Correia, "Thermoelectric micro converters for cooliing and energy-scavenging systems," J. Micromech. Microeng., Vol.18, pp. 064008-1-064008-5, 2008.

[28] J. P. Carmo, J. F. Ribeiro, M. F. Silva, L. M. Goncalves, and J. H. Correia, "Thermoelectric generator and solid-state battery for stand-alone microsystems," J. Micromech. Microeng., Vol.20, pp. 085033-1-, 2010.

Name:
Mizue Mizoshiri

Affiliation:
Assistant Professor, Department of Micro-Nano Systems Engineering, Graduate School of Engineering, Nagoya University

Address:
Furo-cho, Chikusa-ku, Nagoya, Aichi 464-8603, Japan

Brief Biographical History:
2008-2010 Research Fellow of the Japan Society for the Promotion of Science
2010-2013 Research Scientist, National Institute of Advanced Industrial Science and Technology
2013- Assistant Professor, Nagoya University

Main Works:
• "Direct patterning of Cu microstructures using femtosecond laser-induced CuO nanoparticle reduction," Japanese Journal of Applied Physics, Vol.54, No.6S1, Jun. 2015.
• "Lift-off patterning of thermoelectric thick films deposited by a thermally assisted sputtering method," Applied Physics Express, Vol.7, art.no.057101, Jul. 2014.

Membership in Academic Societies:
• Japan Society of Applied Physics (JSAP)
• Japan Laser Processing Society (JLPS)
• Japan Society of Mechanical Engineers (JSME)

Name:
Masashi Mikami

Affiliation:
Research Scientist, Inorganic Functional Materials Research Institute, National Institute of Advanced Industrial Science and Technology

Address:
Furo-cho, Chikusa-ku, Nagoya, Aichi 464-8603, Japan

Brief Biographical History:
2004-2005 Research Fellow of the Japan Society for the Promotion of Science
2005- Research Scientist, National Institute of Advanced Industrial Science and Technology

Main Works:
• "Evaluation of the thermoelectric module consisting of W-doped Heusler Fe_2VAl alloy," Journal of Electronic Materials, Vol.43, pp. 1922-1926, 2014.

Membership in Academic Societies:
• Japan Society of Applied Physics (JSAP)
• Thermoelectric Society of Japan (TSJ)

Name:
Kimihiro Ozaki

Affiliation:
Principal Research Manager, Inorganic Functional Materials Research Institute, National Institute of Advanced Industrial Science and Technology

Address:
2266-98, Anagahora, Moriyama-ku, Nagoya, Aichi 463-8560, Japan

Brief Biographical History:
1994-2001 Research Scientist, National Industrial Research Institute of Nagoya
2001- Senior Researcher, National Institute of Advanced Industrial Science and Technology

Main Works:
• "Microstructural behavior on particle surfaces and interfaces in $Sm_2Fe_{17}N_3$ powder compacts during low-temperature sintering," JMMM, 324-15, 2336-2341, 2012.

Membership in Academic Societies:
• Japan Institute of Metals and Materials (JIM)